Hydrothermal Corrosion Behaviors of Constituent Materials of SiC/SiC Composites for LWR Applications

Shoko Suyama *, Masaru Ukai, Megumi Akimoto, Toshiki Nishimura and Satoko Tajima

Toshiba Energy Systems & Solutions Corporation, Yokohama 230-0045, Japan; masaru.ukai@toshiba.co.jp (M.U.); megumi.akimoto@toshiba.co.jp (M.A.); toshiki1.nishimura@toshiba.co.jp (T.N.); satoko.tajima@toshiba.co.jp (S.T.)

* Correspondence: shoko.suyama@toshiba.co.jp

Abstract: The corrosion behaviors of SiC/SiC composite constituent materials in pure water at operating conditions, such as 300 °C and 8.5 MPa, were studied for potential application in accident-tolerant light water reactor (LWR) fuel cladding and core structures. Five kinds of SiC fibers, four kinds of SiC matrices, and three kinds of fiber/matrix interphase materials were examined in autoclaves. The potential constituent materials for future use in SiC/SiC composites were selected by considering corrosion rates and residual strength characteristics. The mass changes and the residual strength of each specimen were measured. SEM images of the surface layers were also inspected. The SiC fibers, regardless of their purity, crystallinity or stoichiometric ratio, decreased in strength due to the hydrothermal corrosion. For its part, the hydrothermal corrosion resistance of CVD-SiC, as a SiC matrix, was found to be affected by manufacturing conditions such as raw material gas type and synthesis temperature, as well as post-machining morphology. The CVD-carbon (CVD-C), as a fiber/matrix interphase material, showed good hydrothermal corrosion resistance. In order to protect the SiC fibers and the SiC matrices from hydrothermal corrosion, it would appear to be necessary to apply a dense CVD-C coating to both every fiber and the entire surface of the SiC matrices.

Keywords: silicon carbide; fiber; matrix; interphase material; hydrothermal corrosion

1. Introduction

Fiber-reinforced ceramic matrix composites are some of the most promising materials for high-temperature structural applications. Silicon carbide matrix composites are being considered for use as a material for hot section parts of jet engines and gas turbines, and for fusion structural materials [1–3]. Recent high-profile events, such as the incident at the Fukushima Daiichi nuclear power plant, have turned attention to SiC/SiC composites as potential candidates for structural materials to be used in accident-tolerant fuel (ATF) systems of light water reactor (LWR) applications [4–11]. In the incident at the Fukushima Daiichi nuclear power plant, the oxidation of metallic components in high-temperature steam generated hydrogen and caused the explosion of the reactor building. In order to reduce the probability of such hydrogen explosions in the future, SiC/SiC composites are being seriously considered for their effectiveness and accident tolerant properties [6–8]. In addition, many research institutions and industry leaders have formed collaborative teams to start ATF development programs in order to apply SiC/SiC composites to LWR applications [8–10]. Toshiba has started designing materials for applying the SiC/SiC composites to the accident-tolerant LWR fuel cladding and core structures and has been developing process technologies for thin-walled and elongated CVI-SiC/SiC-based tubes and boxes [5,6]. Small-scale prototypes of thin-walled CVI-processed SiC composite tubes and boxes made from SiC fibrous pre-forms have been fabricated [6,8].

Although many studies on the hydrothermal corrosion characteristics of SiC/SiC composites have been conducted, the hydrothermal corrosion of SiC/SiC composites remains among the various feasibility issues that have not yet been fully addressed [6–8,10,12–15]. In particular, how the hydrothermal corrosion resistance of each constituent material affects the overall hydrothermal corrosion of SiC/SiC composites remains unclear.

Firstly, as for SiC fibers, although there are SiC fibers of varying purity, crystallinity, and stoichiometric ratio, it is not yet clear how they differ in terms of corrosion resistance [16–18]. Secondly, as for SiC matrices, high purity grade SiCs have been shown to be more resistant to corrosion but dissolved oxygen in the water accelerated corrosion [12,13,19]. The SiCs appeared to corrode by way of forming silica on the surface and silica dissolving in water at about 300 °C [14]. Namely, the corrosion behavior of high purity grade SiCs is not yet entirely clear. Finally, the hydrothermal corrosion behavior of fiber/matrix interphase materials, such as CVD-Cs and CVD-BNs that have been commonly applied in SiC/SiC composites, also remains unclear [1–3,20].

In this study, candidate constituent materials for SiC/SiC composites, such as SiC fibers, SiC matrices, and fiber/matrix interphase materials, were examined in pure water at operating conditions such as 300 °C and 8.5 MPa to determine the optimal constituent materials for preventing or minimizing hydrothermal corrosion of SiC/SiC composites.

2. Materials

There are three main types of SiC matrix fabrication processes of SiC/SiC composites: chemical vapor infiltration (CVI), precursor impregnation and pyrolysis (PIP), and melt infiltration (MI). The CVI process forms a highly pure, stoichiometric and polycrystalline SiC matrix at lower process temperatures which allows SiC fibers to be used without degradation. Generally, the densification rate is slow and leaves an unavoidable final porosity due to the infiltration of a gas phase SiC precursor. This forms a porous SiC matrix which has a relatively high residual porosity (>10 vol.%) [1–3,21]. Some issues related to the infiltration of a gas phase precursor include limits in terms of scaling and shaping capabilities during the manufacturing process. However, this process is suitable for forming thin-walled structures, such as the channel box (rectangular structure with thin walls) and the cladding tube (cylindrical structure with thin walls). For the reasons stated above, the CVI process is an effective method for producing SiC/SiC composites that satisfy the requirements of core structures, though issues relating to hydrothermal corrosion, porosity, scalability, and manufacturing costs remain [5].

Specimens of five kinds of SiC fibers ("Hi-Nicalon Type S", "Hi-Nicalon", "Tyranno fiber SA", "Tyranno fiber ZMI", "Tyranno fiber LoxM"), four kinds of SiC matrices (CVD-SiCs) and three kinds of fiber/matrix interphase materials (CVD-C and two kinds of CVD-BNs) were prepared. These specimens are shown in Table 1. Product names may be trademarks of their respective companies.

Table 1. Specimens for hydrothermal corrosion test.

Constituent Material	Candidates	Dimensions and Quantities
SiC fiber	"Hi-Nicalon Type S" (NGS) "Hi-Nicalon" (NGS) "Tyranno fiber SA" (Ube) "Tyranno fiber ZMI" (Ube) "Tyranno fiber LoxM" (Ube)	φ12 µm × 500 filaments/strand × 10 m φ14 µm × 500 filaments/strand × 10 m φ10 µm × 800 filaments/strand × 10 m φ11 µm × 800 filaments/strand × 10 m φ11 µm × 800 filaments/strand × 10 m
SiC matrix	CVD-SiC (Morgan) CVD-SiC (Admap) CVD-SiC (Prototype 1) CVD-SiC (Prototype 2)	3 × 4 × 40 mm (Bulk) × 6 p 3 × 4 × 40 mm (Bulk) × 6 p 3 × 4 × 40 mm (Bulk) × 6 p 3 × 4 × 40 mm (Bulk) × 6 p
Fiber/matrix interphase material	CVD-C (Ibiden) CVD-BN (Momentive) CVD-BN (Shin-Etsu)	40 µm coating on 3 × 4 × 40 mm graphite × 6 p 3 × 4 × 40 mm (Bulk) × 6 p 3 × 4 × 40 mm (Bulk) × 6 p

The "Hi-Nicalon Type S" and "Hi-Nicalon" fibers are the product of NGS Advanced Fibers, and "Tyranno fiber SA", "Tyranno fiber ZMI", and "Tyranno fiber LoxM" are the product of Ube Industries. The "Hi-Nicalon", "Tyranno fiber ZMI", and "Tyranno fiber LoxM" fiber specimens were selected for this study for comparison purposes [22,23]. Each SiC fiber specimen tested was a strand with a length of 10 meters. The length was enough to make the specimens for both the tensile strength tests and linear density measurements after the corrosion tests.

The four kinds of CVD-SiC specimens tested consisted of 3 × 4 × 40 mm plates of bulk materials; one type was a product of Morgan Technical Ceramics, one type was a product of Admap, and two of the specimen prototypes were fabricated for this study using different raw material gases and by adjusting CVD synthesis temperatures. All the CVD-SiC specimens were confirmed to be pure and stoichiometric β-SiC crystals [24,25].

A 40 µm thick layer of Ibiden-dense CVD-C coating was applied to a 3 × 4 × 40 mm graphite base material. Two kinds of dense, high-purity CVD-BN specimens by Momentive Performance Materials and Shin-Etsu Chemical were made into 3 × 4 × 40 mm plates of bulk materials. The CVD-BN specimens were selected for this study for comparison purposes [22,26].

3. Experiments

Corrosion tests were examined in pure water at 300 °C and 8.5 MPa in 7.3 liter autoclaves. At this temperature and pressure, the amount of dissolved oxygen in the water was approximately 8 ppm and the pH was between 6 and 7. The exposure times were 0 h, 20 h, and 40 h (JIS R 1647). Before the tests of the SiC fibers were conducted, the sizing agents were eliminated by soaking each fiber specimen in 90 °C water. For each specimen, mass and/or strength were measured before and after the corrosion test.

The tensile strengths of the "Hi-Nicalon Type S" and "Hi-Nicalon" made by NGS Advanced Fibers were tested before and after the corrosion tests using fiber strands with resin ($n = 5$) (JIS R 1657, ISO deliberations). As for the "Tyranno fiber SA", "Tyranno fiber ZMI", and "Tyranno fiber LoxM" specimens made by Ube Industries, the tensile strengths before the corrosion tests were tested using fiber strands with resin ($n = 5$) and mono-filament ($n = 20$) and after the corrosion tests using mono-filament ($n = 20$) (JIS R 1657). The SEM images of the surface layers were also taken, and auger electron spectroscopy (AES) depth analyses were conducted on the SiC fibers. The linear density (TEX) of each fiber before and after the corrosion tests were measured using a strand 1 m in length ($n = 3$) and thickness loss for each fiber was calculated from the linear density measurement.

As for the CVD-SiCs, the four-point bending strength before and after the corrosion tests was tested using a 3 × 4 × 40 specimen ($n = 5$) (JIS R 1601, ISO 14704). The SEM images of the surface layers were taken.

4. Results and Discussion

4.1. SiC Fiber

Tensile strengths of five kinds of SiC fibers before and after the corrosion tests are shown in Figure 1. The strengths of all SiC fibers regardless of their purity, crystallinity or stoichiometric ratio were degraded by hydrothermal corrosion in 300 °C and 8.5 MPa water from a very early stage. The initial strengths of both the "Hi-Nicalon Type S" and "Hi-Nicalon" specimens were over 4 GPa, which was higher than specified in commercial data. The residual strengths of the "Hi-Nicalon Type S" and "Hi-Nicalon" specimens decreased proportionally to the exposure time and showed 74% and 71% of their initial strengths after 40 hours, respectively. Nevertheless, the residual strengths of the "Hi-Nicalon Type S" and "Hi-Nicalon" specimens remained above 3 GPa. On the other hand, the residual strength of the "Tyranno fiber SA", "Tyranno fiber ZMI", and "Tyranno fiber LoxM" specimens dropped once from 0 to 20 hours but then maintained 67%, 87%, and 87% of their initial strengths, respectively, from 20 to 40 hours.
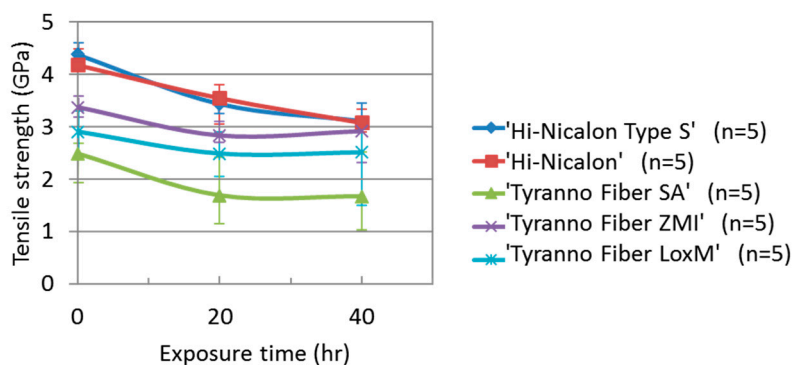
Figure 1. Degradation of tensile strength due to the corrosion test for the five kinds of SiC fibers.

Microphotographs of the surface morphology of the "Hi-Nicalon Type S" and "Hi-Nicalon" SiC fiber specimens before and after the corrosion tests are shown in Figure 2. There was no change in surface morphology observed in the "Hi-Nicalon" specimen, whereas the surface of the "Hi-Nicalon Type S" specimen was slightly less smooth after the test. Thickness losses of each specimen were calculated from linear density measurements and were found to be 135 nm and 193 nm for the "Hi-Nicalon Type S" and "Hi-Nicalon" specimens, respectively (Table 2). This suggests that the decrease in SiC fiber strength was related to their thickness losses as a result of the corrosion.
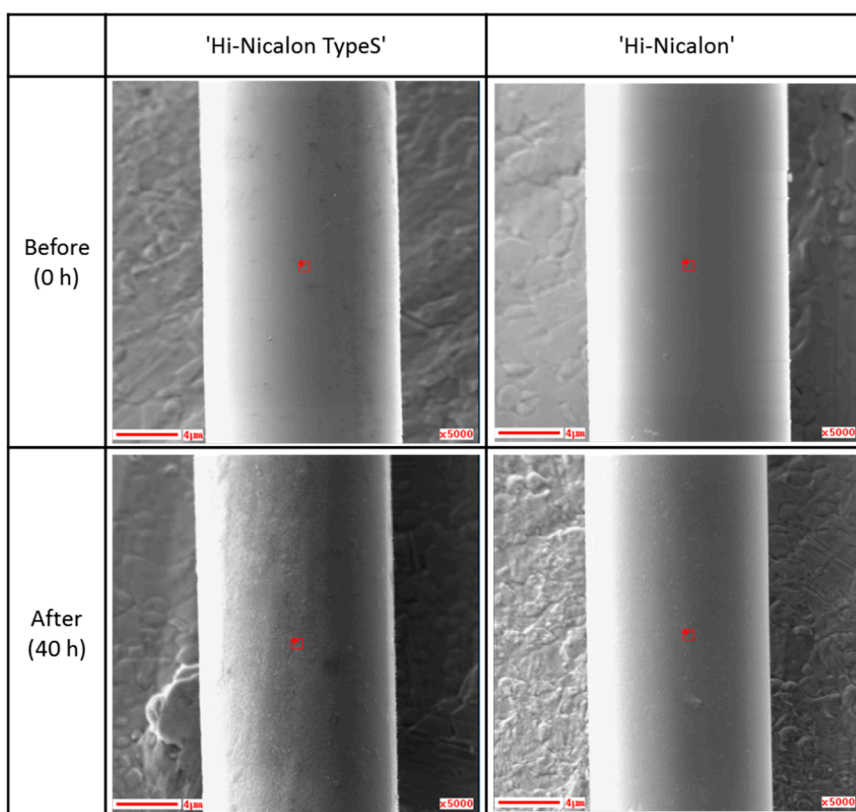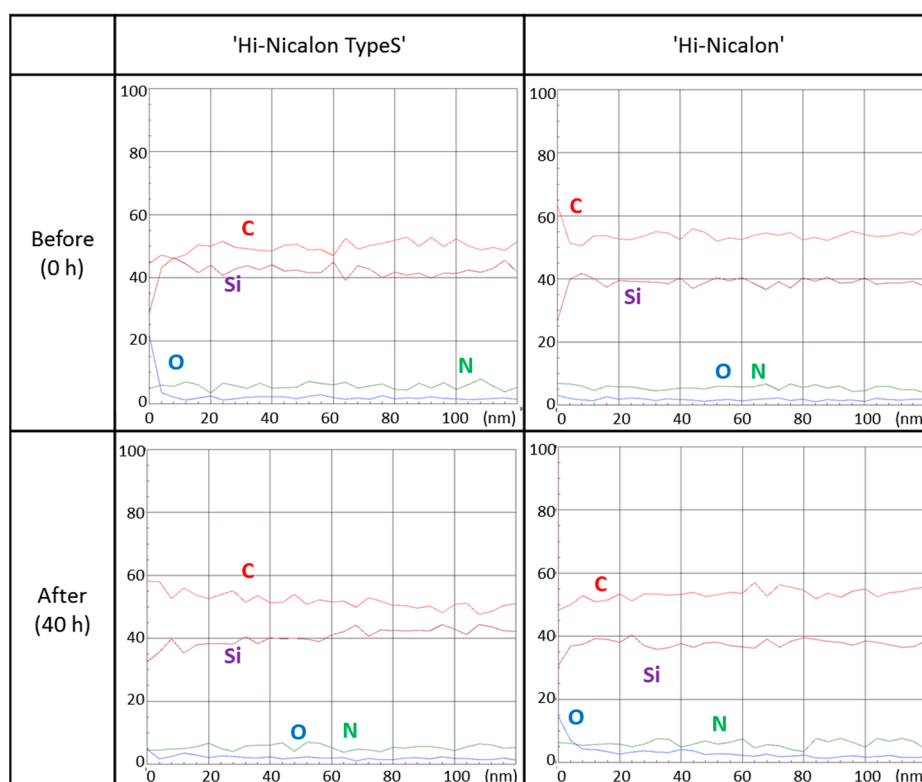

Figure 2. Surface morphology of SiC fibers before and after corrosion tests.

Table 2. Change in the linear density and diameter due to the corrosion tests on the SiC fibers.

SiC Fiber		0 h	20 h	40 h
"Hi-Nicalon Type S"	Linear density (g/km)	194.9	188.9	186.9
	Thickness loss (nm)	0	101	135
"Hi-Nicalon"	Linear density (g/km)	199.7	198.5	194.3
	Thickness loss (nm)	0	21	193

As shown in Figure 3, the composition differed between the surface and the inside of the fibers. The surface composition of both fibers changed after the tests. Although the initial oxygen content of the "Hi-Nicalon Type S" specimen was up to 20% within the top 5 nm of the surface, it decreased to almost 0%, whereas the carbon content increased from 45% to almost 60% after the test. On the other hand, although the initial carbon content of the "Hi-Nicalon" specimen was over 60% within the top 5 nm of the surface, it decreased to below 50%, and the oxygen content increased from almost 0% to 15% after the test. In both types, surface compositions differed from those of the inner fibers as a result of the corrosion tests. The compositional changes observed at the surface suggest that these changes were responsible for some type of hydrothermal oxidation occurring on the surface of the fiber. Furthermore, the thickness of the hydrothermal oxidation layer was found to be extremely thin. That is, the hydrothermal oxidation layer appeared to dissolve in 300 °C and 8.5 MPa water.

Figure 3. Auger electron spectroscopy (AES) analysis results near the surface of the SiC fibers before and after corrosion tests.

As a result, all the SiC fibers, regardless of their purity, crystallinity or stoichiometric ratio decreased in strength due to the hydrothermal corrosion from a very early stage. The SiC fibers would not normally be exposed to water should SiC/SiC composites be applied in LWR applications, since the fibers would be embedded in a SiC matrix. However, there could be the possibility that water might penetrate into the porous SiC matrix from initial cracks. These results suggest that, in order to use

these fibers in LWR applications, it would be necessary to apply a corrosion-resistant coating to every fiber to protect them from hydrothermal corrosion.

4.2. SiC Matrix

The corrosion behavior of four kinds of CVD-SiC specimens is shown in Figure 4. All CVD-SiC specimens showed mass loss in 300 °C and 8.5 MPa water. However, the amount of mass loss differed significantly depending on their CVD-SiC fabrication conditions. The least corrosion mass change was observed in the Admap specimen, followed by the Morgan specimen, the prototype-1 specimen, and the prototype-2 specimen. It is important to note that the corrosion in the Admap and prototype-1 specimens appeared to be decelerating and might plateau.
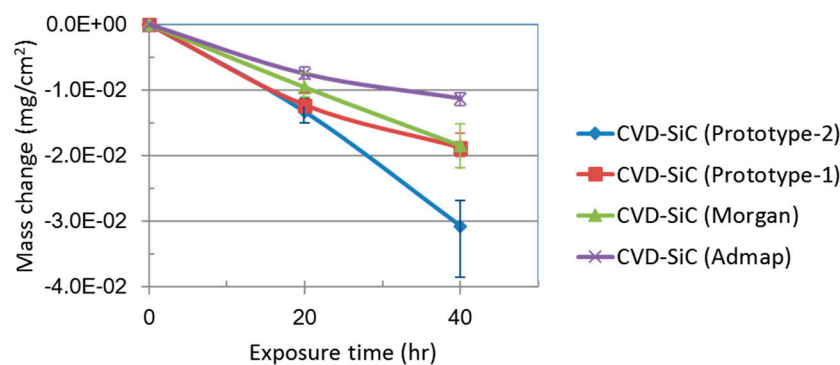

Figure 4. Mass change due to the corrosion tests of four kinds of CVD-SiC specimens.

The following is an equation of the hydrothermal corrosion of SiC in 300 °C water [14]:

$$SiC + 2H_2O = SiO_2 + CH_4 \tag{1}$$

$$SiO_2 + 2H_2O = Si(OH)_4 \tag{2}$$

That is to say, sections of the SiC specimens were found to corrode by way of forming silica and, subsequently, silica dissolving in water.

The surface morphology of the CVD-SiC specimens before and after the corrosion tests suggests that the scratches due to the surface machining could promote corrosion. As shown in Figure 5, underlying residual machined scratches became starting points for corrosion. These scratches appeared after surface layers dissolved in 300 °C and 8.5 MPa water. The presence of etched microstructures with grain boundaries in the images taken after the tests suggests the grain boundary could be also a starting point for corrosion [12,13,19].

Figure 6 shows the bending strengths of the four kinds of CVD-SiC specimens before and after the corrosion tests. Three of the specimens maintained their initial strengths, though that of prototype-2 increased by slightly less than 200 MPa as shown in Figure 6. This phenomenon seemed to be attributed to the dulling of the cracks by the corrosion.
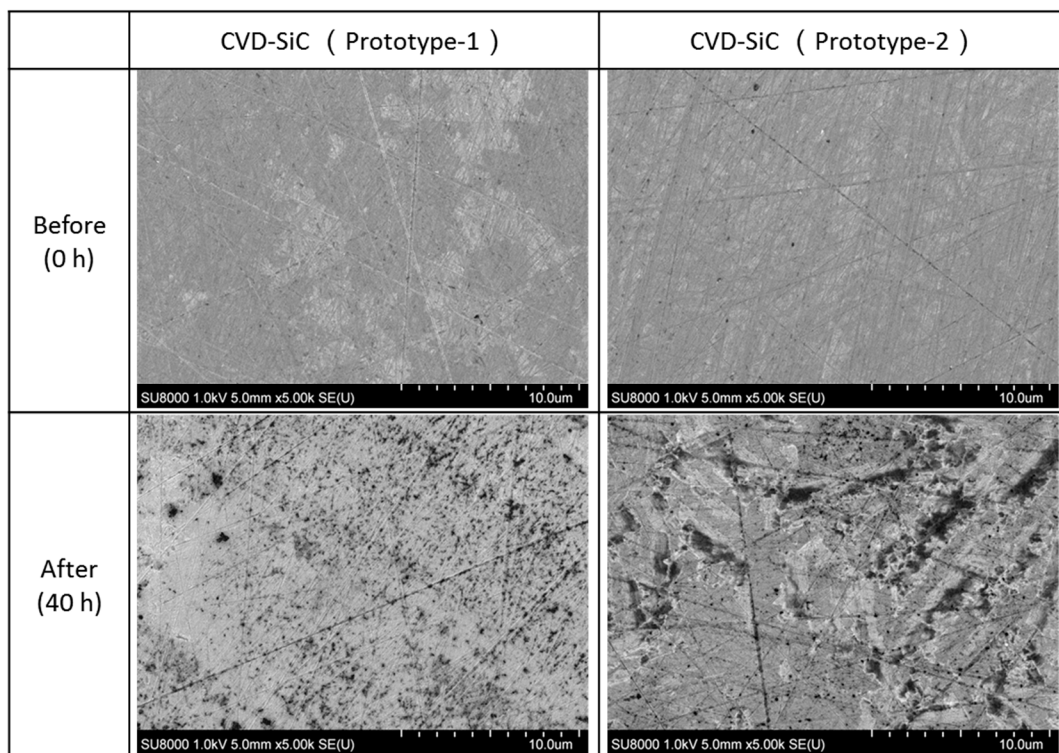
Figure 5. Surface morphology of CVD-SiC specimens before and after corrosion tests.
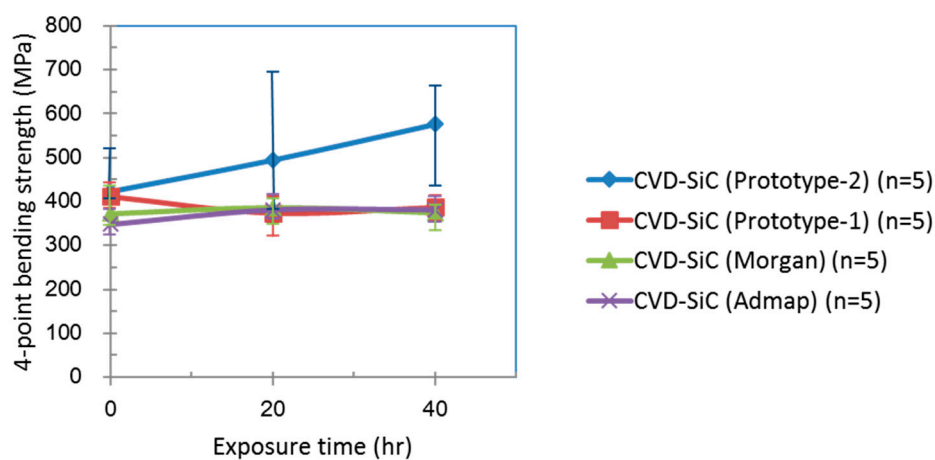

Figure 6. Change in the bending strengths due to the corrosion tests for the four kinds of CVD-SiC specimens.

The hydrothermal corrosion resistance of the CVD-SiC specimens appeared to be affected by manufacturing conditions such as raw material gas type and CVD synthesis temperature as well as post-machining morphology. Optimal CVD manufacturing conditions were found to be essential in order to decrease or minimize this corrosion. These results imply that improvements in these conditions should lead to increased hydrothermal corrosion resistance. If optimal conditions have yet to be determined, these results suggest that it would be necessary to apply a dense corrosion-resistant coating to the entire surface of the SiC matrices as well as the SiC fibers to protect them from hydrothermal corrosion. Future work evaluating the corrosion resistance of CVD-SiCs under different pressure conditions may be necessary to optimize the manufacturing conditions of SiC matrices for use in different LWR applications.

4.3. Fber/Matrix Interphase Material

The corrosion behavior of the two kinds of interphase constituent materials is shown in Figure 7. As shown in Figure 7, the CVD-C coating specimen exhibited good corrosion resistance at 300 °C and 8.5 MPa. This is consistent with results obtained previously in which dense graphite carbon provided superb hydrothermal corrosion resistance in water up to about 400 °C [19,26]. On the other hand, CVD-BN specimens from Momentive Performance Materials exhibited significant mass loss with exposure time which is consistent with results obtained previously with sintered BN containing impurities [20]. All CVD-BN specimens from Shin-Etsu dissolved after 20 hours and are not shown in Figure 7.
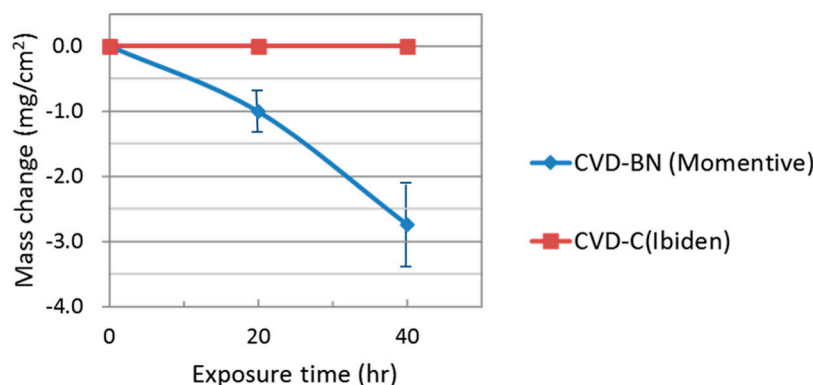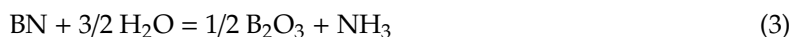

Figure 7. Mass change of two kinds of Interphase material in 300 °C and 8.5 MPa water.

The following is an equation for the hydrothermal corrosion of powders and sintered bodies of hexagonal BN [20]:

$$BN + 3/2\, H_2O = 1/2\, B_2O_3 + NH_3 \tag{3}$$

That is to say, dense CVD-BNs were found to corrode by way of forming boric oxide and ammonia which both dissolved in water at 300 °C and 8.5 MPa.

As a result, a dense CVD-C coating was found to be suitable for fiber/matrix interphase materials in CVI-SiC/SiC composites for LWR applications. Namely, this dense CVD-C coating would act as a fiber/matrix interphase in addition to providing corrosion protection. In order to achieve this, it would be necessary to apply a dense CVD-C coating to the entire surface of every individual fiber. Moreover, there is a possibility that applying a dense CVD-C coating to the entire surface of the SiC matrix would further protect it from hydrothermal corrosion.

5. Conclusions

In this study, the hydrothermal corrosion behaviors of constituent materials of SiC/SiC composites were evaluated in order to determine which would be optimal for future use in LWR applications. Candidate constituent materials, such as SiC fibers, SiC matrices, and fiber/matrix interphase materials, were examined in pure water at operating conditions such as 300 °C and 8.5 MPa at approximately 8 ppm of dissolved oxygen.

The tested SiC fibers, regardless of their purity, crystallinity or stoichiometric ratio, were degraded by hydrothermal corrosion in 300 °C and 8.5 MPa water from a very early stage. The hydrothermal corrosion resistance of CVD-SiC specimens was affected by manufacturing conditions such as raw material gas type and CVD synthesis temperature as well as post-machining morphology. Optimal CVD manufacturing conditions were found to be essential in order to decrease or minimize this corrosion. These results imply that improvements in these conditions should lead to increased hydrothermal corrosion resistance.

On the other hand, the CVD-C coating, as an interphase material, exhibited good corrosion resistance in 300 °C and 8.5 MPa water. It was confirmed that dense graphite carbon provided good

hydrothermal corrosion resistance in 300 °C and 8.5 MPa water. These results suggest that in order to use these materials in LWR applications, it would be necessary to apply a dense CVD-C coating to every individual fiber and the entire surface of SiC matrix to protect them from hydrothermal corrosion.

Author Contributions: Supervision, M.U.; project administration, S.T.; conceptualization, S.S.; validation, S.S., M.A. and T.N.; investigation, S.S, M.A. and T.N.; writing—original draft preparation, S.S.; writing—review and editing, S.S., M.U., M.A., T.N. and S.T.

References

1. Kameda, T.; Suyama, S.; Itoh, Y.; Nishida, K.; Ikeda, I.; Hijikata, T.; Okamura, T. Development of Continuous Fiber-Reinforced Reaction Sintered Silicon Carbide Matrix Composite for Gas Turbine Hot Parts Application. In *ASME Turbo Expo 2000: Power for Land, Sea, and Air*; American Society of Mechanical Engineers Digital Collection: New York, NY, USA, 2000.

2. Kagawa, Y. Thermal shock damage of two-dimensional woven sic fiber-reinforced sic matrix composite. *Compos. Sci. Technol.* **1997**, *57*, 607–611. [CrossRef]

3. Katoh, Y.; Ogawa, K.; Shih, C.; Nozawa, T.; Shinavski, R.J.; Hasegawa, A.; Snead, L.L. Continuous SiC fiber, CVI SiC matrix composites for nuclear applications: Properties and irradiation effects. *J. Nucl. Mater.* **2014**, *448*, 448–476. [CrossRef]

4. Kitano, K.; Ukai, M.; Kubo, T. Development of innovative material for nuclear reactor core with enhanced safety. In Proceedings of the LWR Fuel Performance Meeting/TopFuel 2013, Charlotte, North Carolina, 15–19 September 2013; pp. 936–942.

5. Suyama, S.; Ukai, M.; Uchihashi, M.; Heki, H.; Tajima, S.; Okonogi, K.; Kakiuchi, K. Development of accident tolerant SiC/SiC composite for nuclear reactor channel box. In *Ceramic Materials for Energy Applications V: A Collection of Papers Presented at the 39th International Conference on Advanced Ceramics and Composites*; John Wiley & Sons: Hoboken, NJ, USA, 2015; Volume 36, pp. 35–42.

6. Kakiuchi, K.; Okonogi, K.; Uchihashi, M.; Ukai, M.; Sebe, F.; Takeuchi, Y.; Ogawa, T.; Matsumiya, H.; Suyama, S. Progress on ATF development of SiC for LWR. In Proceedings of the Top Fuel 2016: LWR fuels with enhanced safety and performance, Boise, ID, USA, 11–15 September 2016; American Nuclear Society: La Grange Park, IL, USA, 2016; Volume 49.

7. Lahoda, E.; Ray, S.; Xu, P.; Boylan, F.; Jacko, R. SiC cladding corrosion and mitigation. In Proceedings of the Top Fuel 2016: LWR fuels with enhanced safety and performance, Boise, ID, USA, 11–15 September 2016; American Nuclear Society: La Grange Park, IL, USA, 2016; Volume 49.

8. Pasamehmetoglu, K.; Massara, S.; Costa, D.; Bragg-Sitton, S.; Moatti, M.; Kurata, M.; Iracane, D.; Ivanova, T.; Bischoff, J.; Delafoy, C.; et al. *State-of-the-Art Report on Light Water Reactor Accident-Tolerant Fuels*; No.7317; Nuclear Energy Agency of the OECD (NEA): Paris, France, 2018; Available online: https://inis.iaea.org/search/search.aspx?orig_q=RN:50015394 (accessed on 30 September 2019).

9. Deck, C.P.; Jacobsen, G.M.; Sheeder, J.; Gutierrez, O.; Zhang, J.; Stone, J.; Khalifa, H.E.; Back, C.A. Characterization of SiC-SiC composites for accident tolerant fuel cladding. *J. Nucl. Mater.* **2015**, *466*, 667–681. [CrossRef]

10. Yueh, K.; Terrani, K.A. Silicon carbide composite for light water reactor fuel assembly applications. *J. Nucl. Mater.* **2014**, *448*, 380–388. [CrossRef]

11. Sauder, C. Ceramic Matrix Composites: Nuclear Applications. In *Ceramic Matrix Composite: Materials, Modeling and Technology*; Bansal, N.P., Lamon, J., Eds.; Wiley Online Library: Hoboken, NJ, USA, 2014. [CrossRef]

12. Kim, W.-J.; Hwang, H.S.; Park, J.Y.; Ryu, W.-S. Corrosion behaviors of sintered and chemically vapor deposited silicon carbide ceramics in water at 360 °C. *J. Mater. Sci. Lett.* **2003**, *22*, 581–584. [CrossRef]

13. Park, J.Y.; Kim, I.H.; Jung, Y.I.; Kim, H.G.; Park, D.J.; Kim, W.J. Long-term corrosion behavior of CVD SiC in 360 °C water and 400 °C steam. *J. Nucl. Mater.* **2013**, *443*, 603–607.

14. Terrani, K.A.; Yang, Y.; Kim, Y.J.; Rebak, R.; Meyer, H.M., III; Gerczak, T.J. Hydrothermal corrosion of SiC in LWR coolant environments in the absence of irradiation. *J. Nucl. Mater.* **2015**, *465*, 488–498. [CrossRef]

15. Lorrette, C.; Sauder, C.; Billaud, P.; Hossepied, C.; Loupias, G.; Braun, J.; Michaux, A.; Torres, E.; Rebillat, F.; Bischoff, J. SiC/SiC composite behavior in LWR conditions and under high temperature steam environment. In Proceedings of the Top Fuel 2015, Zurich, Switzerland, 13–17 September 2015.

16. Ichikawa, H. Polymer-Derived Ceramic Fibers. *Annu. Rev. Mater. Res.* **2016**, *46*, 335–356. [CrossRef]

17. Ishikawa, T.; Kohtoku, Y.; Kumagawa, K.; Yamamura, T.; Nagasawa, T. High-strength alkali-resistant sintered SiC fibre stable to 2200 °C. *Nature* **1998**, *391*, 773. [CrossRef]

18. Kanno, Y.; Yasuda, E.; Yoshimura, M. Hydrothermal corrosion of Si-Ti-C-O (Tyranno) fibers. *Hyomen Kagaku* **1993**, *14*, 229–235. (In Japanese) [CrossRef]

19. Barringer, E.; Faiztompkins, Z.; Feinroth, H.; Allen, T.; Lance, M.; Meyer, H.; Walker, L.; Lara-Curzio, E. Corrosion of CVD Silicon Carbide in 500 °C supercritical water. *J. Am, Ceram. Soc.* **2007**, *90*, 315–318. [CrossRef]

20. Oda, K.; Yoshio, T. Hydrothermal corrosion of hexagonal boron nitride. *J. Ceram. Soc.* **1993**, *101*, 855–859. (In Japanese) [CrossRef]

21. 21. Suyama, S.; Kamada, T.; Itoh, Y. Evaluation of microstructure for SiC/SiC composites using mercury intrusion method. *J. Ceram. Soc. Jpn.* **2000**, *108*, 854–860. [CrossRef]

22. Chaffron, L.; Sauder, C.; Lorrette, C.; Briottet, L.; Michaux, A.; Gelebart, L.; Coupe, A.; Zabiego, M.; Leflem, M.; Seran, J.-L. Innovative SiC/SiC composite for nuclear applications. In *European Physical Journal Web of Conference*; EDP Science: Julius, France, 2013; Volume 51, p. 01003. [CrossRef]

23. Sauder, C.; Lamon, J. Influence of fiber surface roughness on mechanical behaviour of SiC/SiC minicomposites with Hi-Nicalon S and SA3 reinforcement. In Proceedings of the 35th International Congress on Advanced Ceramic and Composites, Daytona beach, FL, USA, 23–28 January 2011.

24. Hirai, T. Silicon Carbide Prepared by Chemical Vapor Deposition. In *Silicon Carbide Ceramics—1*; Somiya, S., Inomata, Y., Eds.; Springer: Dordrecht, The Netherlands, 1991; Volume 1.

25. Langlais, F.; Loumagne, F.; Lespiaux, D.; Schamm-Chardon, S.; Naslain, R. Kinetic processes in the CVD of SiC from CH3SiCl3-H2 in a vertical hot-wall reactor. *Le Journal de Physique IV* **1995**, *5*, C5-105–C5-112. (In France) [CrossRef]

26. Katoh, Y.; Nozawa, T.; Snead, L.L. Mechanical properties of thin pyrolytic carbon interphase SiC-matrix composites reinforced with near stoichiometric SiC Fibers. *J. Am. Ceram. Soc.* **2005**, *88*, 3088–3095. [CrossRef]